DOI: 10.61782/fa.2023.0232

forum acusticum 2023

DIFFUSE ACOUSTIC REFLECTION

Wolfram Bartolomaeus*
Federal Highway Research Institute, Environmental Protection, Emissions, Germany

ABSTRACT

The Huygens principle was extended to the Huygens-Fresnel Principle by Augustin Fresnel and can be derived directly form a scalar differential wave equation, known as Helmholtz equation. When calculating energy of the scalar field, a factor of obliquity must be added.

The calculation of the sound power reflected by diffuse reflection from a rough surface is particularly simple when using the basic photometric equations for radiation and irradiation.

A geometry of the experimental setup for both, simulation and measurement, are described. The simulations are using Rasmussen's transfer grid method. The idea is to first "store" the energy emitted by the source per solid angle on the reflection surface in a grid. Next, the energy per solid angle received by the receiver from the reflection surface is also "stored" in a grating. In the last step, the energy as a function of travel time is calculated by summing up.

The roughness (texture wavelength and depth) of a surface leads to diffuse reflection. I.e. there is a redistribution of the power in the reflected beam, whereas with non-absorbing surfaces the energy is retained.

Keywords: *diffuse reflection, impulse response, simulation*

1. INTRODUCTION

As early as 1914, Felix Jentsch dealt with the irregular reflection of light on rough or opaque surfaces in his habilitation treatise entitled „Studie über Emission und diffuse Reflexion“ ("Study on Emission and Diffuse Reflection" [1]). Lambert's law of emission can also be found there, which states that the radiant intensity of the light reflected on a diffuse surface is proportional to the cosine of the emission angle. Even if the cosine law is only approximately valid for real material, its simple form makes it well suited for a mathematical description of diffuse reflection.

**Corresponding author*: bartolomaeus@bast.de.

2. THEORETICAL BASICS

2.1 Huygens Principle

Huygens' principle of elementary waves, proposed 1678 by Christiaan Huygens, can be applied to curved wave fronts (Figure 1) as well as to the reflection at surfaces (Figure 2), which can also be uneven.

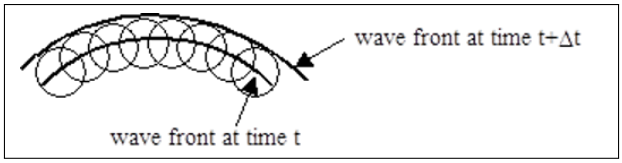

Figure 1. Propagation of a curved wave front within a time step from t to $t + \Delta t$, https://www.mathpages.com/home/kmath242/kmath242.htm

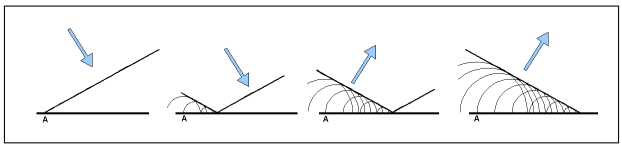

Figure 2. Reflection of a plane wave front at a plane A, https://commons.wikimedia.org/w/index.php?curid=6981543

The Huygens Principle is based on the assumption that at every time instant, every point on a primary wave-

front can be thought of as a continuous emitter of secondary waves (sources) and these secondary waves combine to produce a new wavefront in the direction of propagation.

Specifically in the case of the delta function as an impulse response – i.e. a singularity – an initially frequency-independent approach as in the Biot-Tolstoy-Medwin theory [2] can be used.

2.2 Huygens-Fresnel Principle

The Huygens principle was extended to the Huygens-Fresnel Principle by Augustin Fresnel. The Huygens-Fresnel Principle can be derived directly form a scalar differential wave equation, known as Helmholtz Equation

$$\left(\Delta + k^2\right) U = 0 \tag{1}$$

with suitable boundary conditions by use of Greens Theory

It can be written in the Rayleigh-Sommerfeld form for the diffraction [3]

$$U\left(P_0\right) = \frac{1}{\mathrm{i}\lambda} \iint_{\Sigma} U\left(P_1\right) \frac{e^{\mathrm{i}kr_{01}}}{r_{01}} \cos\Theta ds \tag{2}$$

It describes the amplitude of a scalar field U at a Point P_0 superposed of diverging spherical waves, $e^{\mathrm{i}kr_{01}}/r_{01}$, of wavelength, $\lambda = 2\pi/k$, originating from secondary sources located at Points P_1 within an opening Σ. The distance from the secondary source to the receiver point is denoted by r_{01} and θ is the angle between the normal vector of the opening, $\vec{n}$ and the direction from source to receiver, $\vec{r}_{01}$.

The complex amplitude is proportional to the amplitude at the excitation $U\left(P_1\right)$ at the source points. The amplitude is inversely proportional to the wavelength λ. It has a phase that leads by $90°$ the incident wave and each secondary source has a directivity pattern of $\cos\Theta$. This directivity pattern effects that the propagation of the wavefront is directed forward and no a wavefront propagating in the reverse direction can be observed.

When calculating energy of the the scalar field, a factor of obliquity must be added [4]

$$K\left(\Theta\right) = \frac{1}{2}\left(1 + \cos\left(\Theta\right)\right) \tag{3}$$

Figure 3 shows the directivity of both, Huygens- and Kirchhoff-model.

In nearly direct directions with small angle, $\Theta \approx 0°$, both directivity patterns are nearly the same. At angles

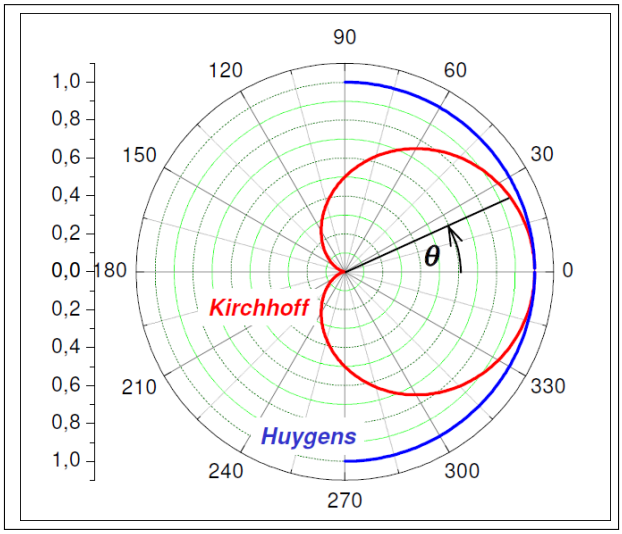

Figure 3. Directivity of Huygens and Kirchhoff from [5]

of 30°, 60° and 90° the deviation of the Kirchhoff-model from the omni-directivity of the Huygens-model is about 5%, 25% and 50%.

The application of the Huygens-Fresnel Principle for modelling acoustical diffraction is described e.g by Kapralos et al. [6]. Experimental results, described there, indicate that the method is capable of modelling acoustical diffraction phenomena in a simple and efficient manner. It should be possible to use it for interactive virtual environments.

Not only the diffraction but also the reflection can be modelled with the Huygens-Fresnel Principle with great efficiency. If the angle of incidence is not to high both, Huygens and Kirchhoff directivity (of Huygens-Fresnel approach) are nearly the same and the more simple omni-directivity of the Huygens-model can be used for simplicity.

2.3 One-Way Wave Equation

A more formal way to get rid of the backward propagation of sound waves is the use of One-Way wave equations [7]. With bulk modulus times displacement $K\vec{\xi}$ the wave equation is

$$\frac{\partial^2}{\partial t^2}\left(K\vec{\xi}\right) - c^2\vec{\nabla}^2\left(K\vec{\xi}\right) = 0 \tag{4}$$

Here c is the velocity of the sound wave.

This second order partial differential equation can be split into two first order partial differential equations

$$\frac{\partial}{\partial t}\left(K\vec{\xi}\right) \pm c\vec{\nabla}\left(K\vec{\xi}\right) = 0 \tag{5}$$

The equation with the negative sign describes a wave, travelling in the outgoing direction. Sound pressure and velocity can be defined as usual

$$p = -\vec{\nabla}\left(K\vec{\xi}\right) = 0 \tag{6}$$

$$\vec{v} = \frac{\partial\left(\vec{\xi}\right)}{\partial t} \tag{7}$$

2.4 Photometric Equation

The calculation of the sound power reflected by diffuse reflection from a rough surface is particularly simple when using the basic photometric equations for radiation and irradiation:

$$d^2\Phi_{1\to 2} = \frac{L_1 \cdot \cos(\beta_1)\cos(\beta_2)\, dA_1 dA_2}{r^2} \tag{8}$$

$$d^2\Phi_{2\leftarrow 1} = \frac{K_2 \cdot \cos(\beta_1)\cos(\beta_2)\, dA_1 dA_2}{r^2} \tag{9}$$

In which mean:

- Φ luminous flux in lm,
- L luminance in $\mathrm{cd\,m^{-2}}$,
- K luminance in $\mathrm{cd\,m^{-2}}$,
- β polar angle of area 1 or 2,
- dA area element of area 1 or 2 in $\mathrm{m^2}$ and
- r distance of surfaces 1 and 2 from each other in m.

Figure 4 shows the geometry underlying the basic photometric equations.

This equation is symmetrical with respect to source and receiver. In order to use it in acoustics, the photometric terms must be converted into acoustic terms. The relations given in the table 1 apply.

The radiometric radiant energy Q_e corresponds to the photometric quantity of light Q_v. The acoustic source strength, the sound flux q, is defined as volume flow per unit of time and only becomes an energetic quantity by multiplication with density and sound velocity of the medium.

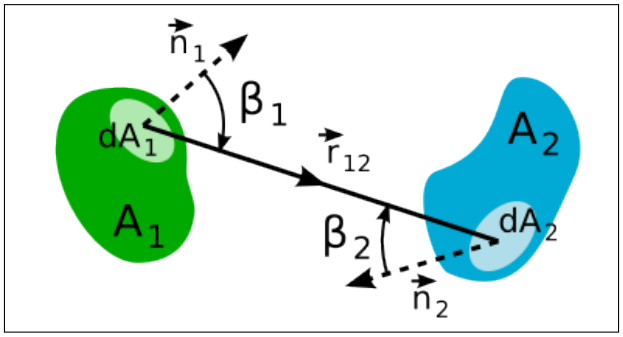

Figure 4. Photometric basic equations for radiation or irradiation (By Cepheiden – Own work, Public domain, https://commons.wikimedia.org/wiki/File:Fotometrisches_Grundgesetz_(Schema)_DE.svg

Table 1. radiometric, photometric and acoustic quantities

kind	entities		
	radio.	foto.	acoust.
source	$[Q_e] = \mathrm{W\,s}$	$[Q_v] = \mathrm{lm\,s}$	$[q] = \frac{\mathrm{m^3}}{\mathrm{s}}$
power	$[\Phi_e] = \mathrm{W}$	$[\Phi_v] = \mathrm{lm}$	$[P] = \mathrm{W}$
radiance	$[L_e] = \frac{\mathrm{W}}{\mathrm{m^2}}$	$[L_v] = \frac{\mathrm{cd}}{\mathrm{m^2\,rad}}$	$[B] = \frac{\mathrm{W}}{\mathrm{m^2 s}}$

For the power quantities, radiant flux Φ_e, luminous flux Φ_v and sound power P correspond to each other. In photometry, however, the unit is lumen (lm) instead of watt (W).

In radiance, there is the radiometric luminance L_e and the photometric radiance L_v. The former refers to an illuminated or luminous surface, while the latter refers to area and solid angle. Kuttruff [8] gives an analogous formula to (9) for acoustical irradiation and defines the irradiation strength B as a measure of the acoustical radiance.

In particular, the photometric reference to the solid angle seems helpful for the following considerations of diffuse acoustic reflection.

3. SETUP

3.1 Geometry

The geometry of the symmetrical experimental setup for both, simulation and measurement, is described as follows:

- d_{QE} = 1,000 m distance source – receiver
- h = 0,866 m height source and receiver above ground
- ϕ = 30° inclination source to receiver

This results in further geometrical parameters:

- $d_{Q'E}$ = 2,000 m distance mirror source – receiver
- α = 60° inclination mirror source to receiver

A three-dimensional view of the geometry of the symmetrical experimental setup is shown in Figure 5.

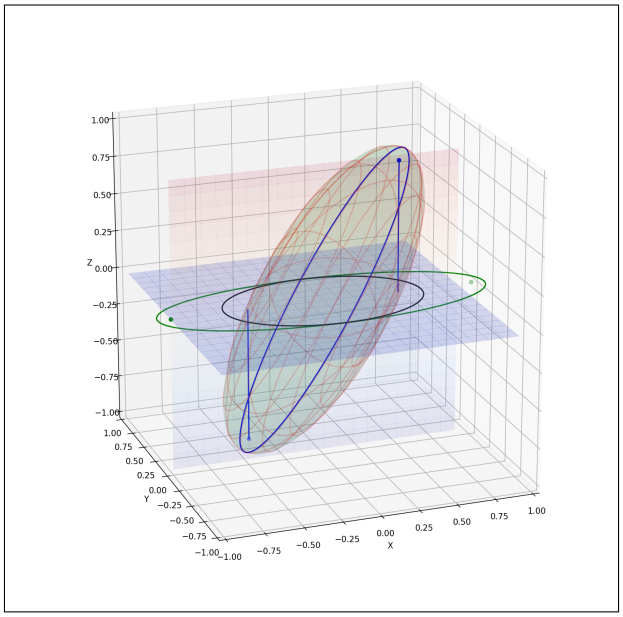

Figure 5. Three-dimensional view of the geometry of the symmetrical experimental setup with position of mirror source and receiver (dots at vertical lines) and the resulting ellipsoid constructed from a (large) rotated ellipse in the plane at $z = 0$ and the (small) ellipse resulting from the intersection with the plane at $z = 0$

The sound power that arrives at the receiver at a given time comes from sound rays that, starting from the mirror source, touch the ellipsoid of rotation. The size of the ellipsoid depends on the given travel time of the sound rays. The intersection of the ellipsoid with the reflection plane is an ellipse. All sound rays that are reflected on the edge of this ellipse arrive at the receiver at the specified time.

Figure 6 shows the experimental setup in the Hall for Acoustic Model Technology (HaMt).

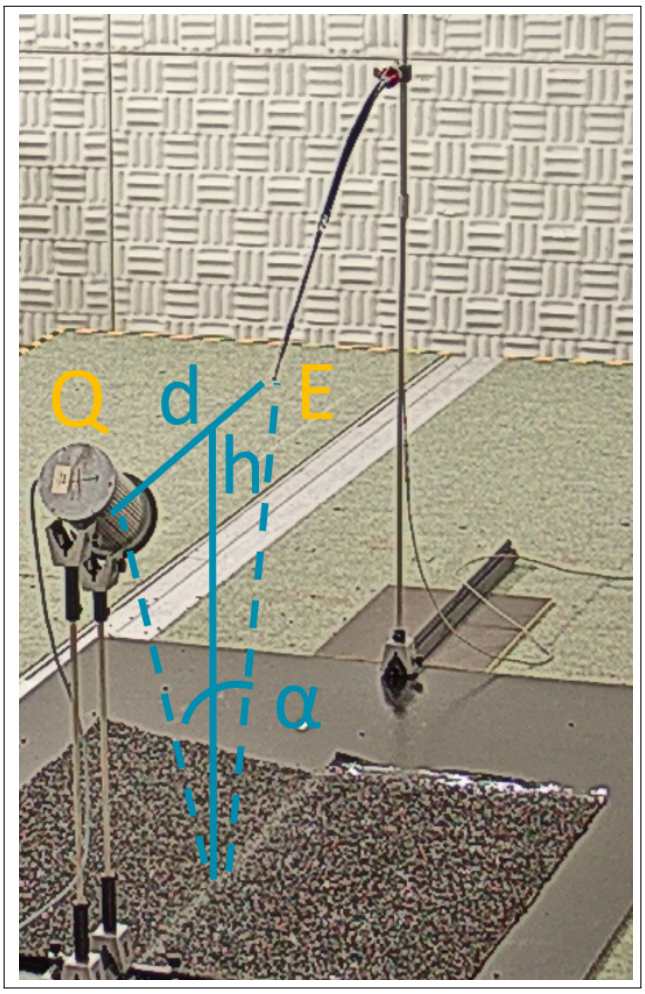

Figure 6. experimental set-up in the Hall for Acoustic Modelling (HaMt)

The reflection plane here is covered with MR 3 rolled asphalt from Moquette routière with a grain size of 6/8 mm.

3.2 Simulation

The simulations were programmed in Python and Rasmussen's transfer grid method was used [9]. The idea is to first "store" the energy emitted by the source per solid angle on the reflection surface in a grid. This corresponds to equation (1). Next, the energy per solid angle received by the receiver from the reflection surface is also "stored" in a grating. This corresponds to equation (2).

This method can be stated as an early version of "sonel mapping" [6]. In a first pass (the sonel tracing stage), sound elements known as sonels are emitted from the sound source and traced until they interact with the surface at a point p and the sonel is stored in a structure called a sonel map. In the second stage (the rendering stage), the room impulse response is estimated through the use of the previously constructed sonel map. The impulse response is estimated by emitting acoustic rays from the receiver and tracing them to the surface. The sonel map is used to provide an estimate of the sound energy leaving point p and arriving at the receiver.

The rays can be constructed as pyramids with a triangular base. The summit of the pyramid is at the source or at the receiver and the base is on the transfer grid (sonel map).

In his phd thesis Stephenson uses a similar method of quantised pyramidal rays to calculate the diffraction in room acoustics [10].

The calculation of the solid angles for three given position vectors $\vec{r_1}$, $\vec{r_2}$ and $\vec{r_3}$ is quite simple and is [11]:

$$\Omega = 2 \cdot \arctan\left(\frac{(\vec{r_1}, \vec{r_2}, \vec{r_3})}{|\vec{r_1}| \cdot |\vec{r_2}| \cdot |\vec{r_3}| + (\vec{r_1} \cdot \vec{r_2}) \cdot |\vec{r_3}| + \\ + (\vec{r_1} \cdot \vec{r_3}) \cdot |\vec{r_2}| + (\vec{r_2} \cdot \vec{r_3}) \cdot |\vec{r_1}|}\right) \tag{10}$$

The location vectors point from the source (or the receiver) to a triangular element of the triangulated plane. Two triangles taken together then result in a grid cell.

In the next step, the travel times are determined for each grid cell from the sum of the distances to the source or receiver by multiplication with the speed of sound. These are discretised for a suitable step size depending on an upper cut-off frequency.

If one assumes an isotropic, i. h. spherical, radiated impulse from the source, the grid cells can be assigned to the received signal in time. The energy transmitted in the process results from multiplying the energy previously "stored" in the grating by the source and receiver.

4. EXECUTION

4.1 Measurement

The measurements were made with the following experimental setup:

- Monkey Forest software with ROBO 3 frontend at 96 kHz,
- KEMO filter as high pass from 2 kHz,
- QCS amplifier for the output signal,
- CORONA 514 ion tweeter 3,5 kHz to 120 kHz,
- B&K microphone 4939 and microphone amplifier 2670, 4 Hz to 100 kHz
- B&K Nexus amplifier 2690, 20 Hz to 100 kHz.

The room impulse responses were measured with a sweep. A similar setup was used by Rizzi et al. [12] for the measurement of the uniformity of scattering.

4.2 Simulations

In the simulation, the roughness of the reflection surface was realised by Gaussian noise. Figure 7 shows the nearly circular "illuminated" reflection surface with a radius of about 2 m (which corresponds to a time difference to the first reflection of about 7 ms).

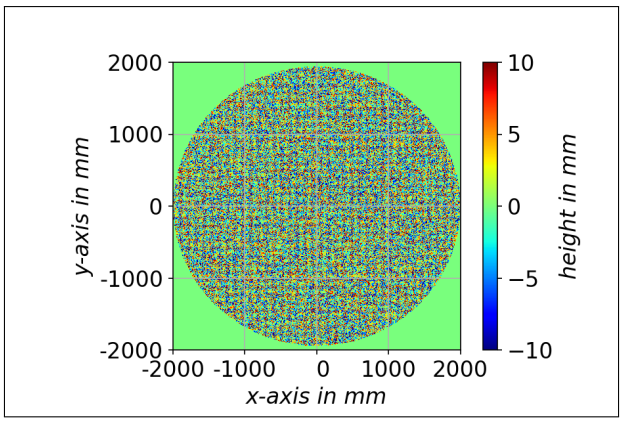

Figure 7. reflective surface with a rough surface modelled by Gaussian noise

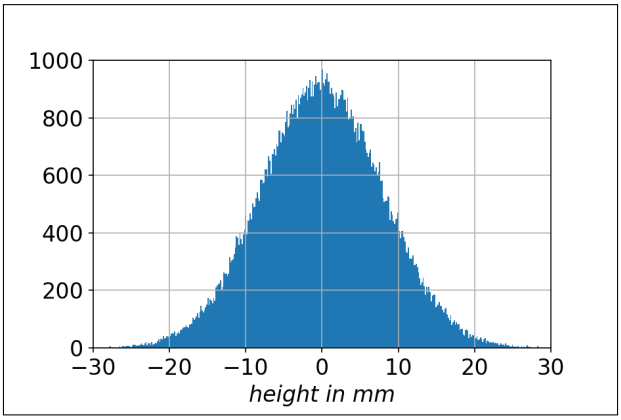

Figure 8. statistical height distribution of the reflecting surface; standard deviation σ = 8 mm

That the roughness follows a Gaussian distribution can be seen in Figure 8.

This is only a rough model of reality since the differences in height from position to position can be very high. A more sophisticated model could make use of an two dimensional autoregressive–moving-average (ARMA) model. Then the autoregression (AR) leads to a fractal surface [13] and the moving average (AM) is limiting the amplitude of the surface. All together it gives a description of a (weakly) stationary stochastic process. But the simple random number model used here is sufficient enough, because strong local variations in texture amplitude are not of interest when calculating illumination and radiation of the surface.

Figure 9 shows the transfer grids for transmitter and receiver without roughness (standard deviation of texture amplitude σ = 0 mm) and Figure 10 for σ = 8 mm.

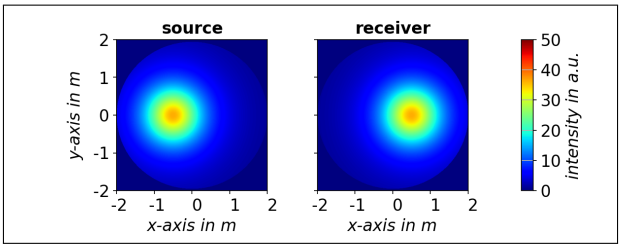

Figure 9. transfer grid for transmitter and receiver; standard deviation of texture amplitude σ = 0 mm

The rough surface results in clearly visible redistributions of both illuminated and radiated energy. Instead of a concentric ring structure, the energy distribution looks like viewed through a fluted glass (also called “light scattering glass”).

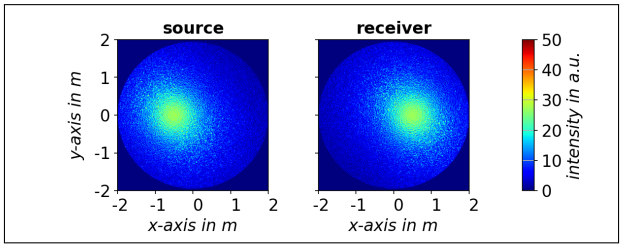

Figure 10. transfer grid for transmitter and receiver; standard deviation of texture amplitude σ = 8 mm

To save computing time, a scaling factor of 10 was used. This shortens the time between the first and diffuse reflection from approx. 7 ms to approx. 0.7 ms.

5. RESULTS AND DISCUSSION

5.1 Measurement Results

The spectrum of a sweep with direct and reflected signal in Figure 11 (smooth) is characterised by strong interference between both signal components compared to the spectrum without reflection (noisy).

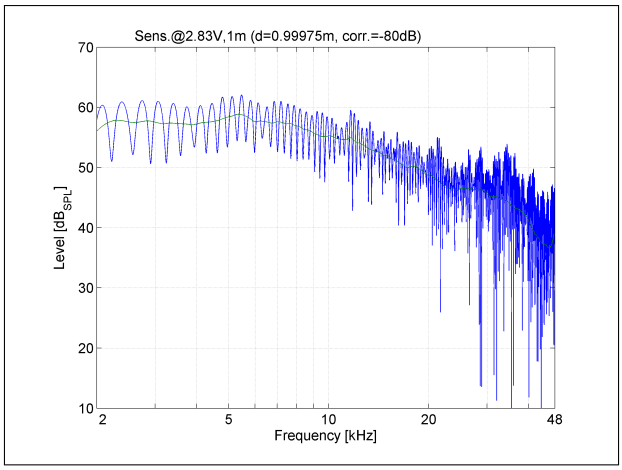

Figure 11. spectrum of the sound pressure level of a measurement without reflection (smooth) and with reflection at a rough plane (noisy) in the range from 2 kHz to 48 kHz

An amplitude modulation of the form $\sin^2(fT)$ with

a time constant of $T \approx 3$ ms. This corresponds to the detour of about 1 m as a difference from reflected path and direct path of the sound.

The Fourier transform of the spectrum is the sought spatial impulse response of the experimental setup under consideration and is shown in Figure 12.

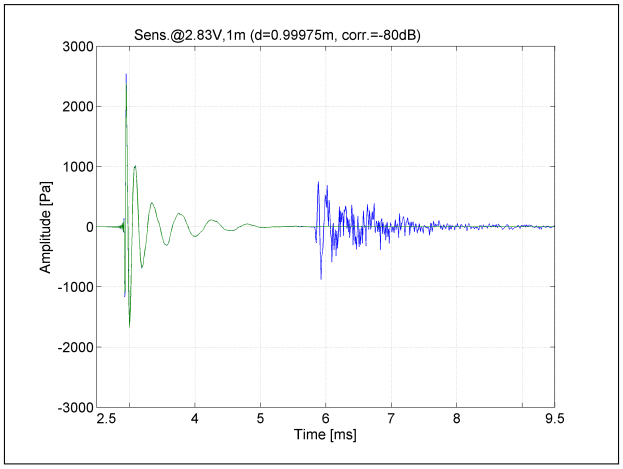

Figure 12. sound pressure amplitude of the room impulse response of direct (smooth ahead) and reflected (noisy behind) sound

The window function of the sweep is "folded" into the direct and the reflected signal respectively. For the direct part of the signal in the time domain up to almost 6 ms, the spatial impulse responses of both spectra from Figure 11 are almost identical.

Compared to the direct signal, which arrives at the receiver after approx. 3 ms (corresponding to the distance of 1 m between source and receiver), the signal reflected at the rough surface, which arrives after approx. 6 ms (corresponding to a distance of 2 m) is, as expected, strongly noisy.

5.2 Discussion

In order to be able to compare simulation and measurement, a representation of the received sound power as a function of the time of flight was chosen. In Figure 13 the simulated and measured sound power (squared sound pressure) of direct sound, reflected sound and their difference is plotted as a function of the time of flight.

Within the achievable accuracy, especially due to the frequency limitation, a high similarity of the signals can

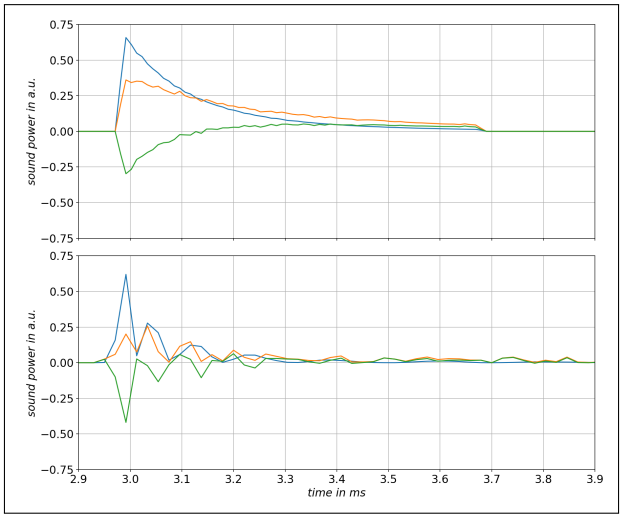

Figure 13. Simulated (top) and measured (bottom) sound power of direct sound (topmost curve), reflected sound (middle curve) and their difference (lowermost curve) as a function of time of flight

be achieved by a suitable choice of the roughness parameter σ. With a standard deviation of the Gaussian distribution of 8 mm, the relative change of the maximum sound power $(P_{refl.} - P_{dir.})/P_{dir.}$ is about 45% and the relative change in sound energy $(E_{refl.} - E_{dir.})/E_{dir.}$ (with $E = \int P dt$) is about 2.5%.

The relative change in sound energy is comparable to the definition of the random-incidence scattering coefficients δ given by Vorländer and Mommertz [14].

The roughness (texture wavelength and depth) of a surface leads to a diffuse reflection. I.e. there is a redistribution of the power in the reflected beam, whereas with non-absorbing surfaces the energy is retained.

6. OUTLOOK

In analogy to the luminance in optics, in acoustics quantities of the sound power per area and solid angle can be calculated [15].

In simulation and measurement methods, the frequency dependence of diffuse reflection can be investigated by applying octave (Figure 14) and third octave filters.

The measurement method is initially limited to reflecting surfaces without absorption. However, an extension of the model to (partially) absorbing material seems

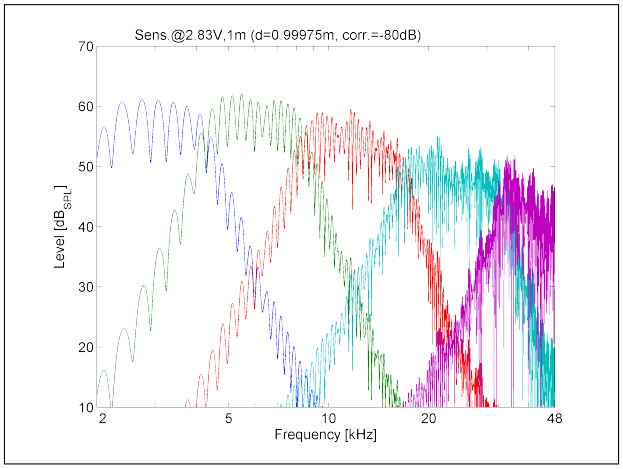

Figure 14. spectrum of the sound pressure level of a measurement with reflection at a rough plane (noisy) in the range from 2 kHz to 48 kHz for oktave bands with middle frequencies of 2, 4, 8 and 16 and 32 kHz

possible. Possibly, however, two microphones would then have to be used as in the NORDTEST method for determining the ground impedance [16].

Likewise, the backscatter of objects (e. g. cylinders) could be calculated and measured. Here a comparison with the BTM theory would be possible [17].

Because of the relative simple two stage calculation method it is possible to use the method described here for virtual reality purposes with respect to the acoustical part. When the source is fixed in respect to the reflecting surface, the first part of calculation, forming the transfer matrix, can be done in advanced. While moving the receiver to different positions the second step of calculation, from transfer matrix to receiver can be carried out either in real time or taken from pre-calculations also.

7. REFERENCES

[1] F. Jentzsch, *Studie über Emission und diffuse Reflexion*. Habilitation, 1914.

[2] M. A. Biot and I. Tolstoy, "Formulation of wave propagation in infinite media by normal coordinates with an application to diffraction," *JASA*, vol. 29, no. 3, pp. 381–391, 1957.

[3] J. W. Goodman, *Fourier Optics*. Roberts and Company Publishers, 2005.

[4] E. Hecht, *Optics*. Pearson Education Inc., 2002.

[5] R. Gross, "Physik III - Optik und Quantenphänomene." Vorlesungsskript WS 2002/2003, Lehrstuhl für Technische Physik der Technischen Universitär München, März 2003.

[6] M. J. B. Karalos and E. Milios, "Acoustical diffraction modelling utilizing the Huygens-Fresnel Principal," in *HAVE 2005 - International Workshop on Haptic Audio Visual Environments and their Applications*, (Ottawa, Ontario, Canada), IEEE, 1-2 October 2005.

[7] O. Bschorr and H.-J. Raida, "Factorized One-Way Wave Equation," *Acoustics*, no. 3, pp. 717–722, 2021.

[8] H. Kuttruff, *Room Acoustics*. London: Spon Press, fourth ed., 2000.

[9] K. B. Rasmussen, "Propagation of road traffic noise over level terrain," *Am.*, no. 29, pp. 381–391, 1982.

[10] U. Stephenson, *Beugungssimulation ohne Rechenzeitexplosion: Die Methode der quantisierten Pyramidenstrahlen – ein neues Berechnungsverfahren für Raumaskustik und Lärmimmissionsprognose*. Ph.D. dissertation, RWTH-Aachen, 2004.

[11] A. van Oosterom and J. Strackee, "The Solid Angle of a Plane Triangle," in *Biomedical Engineering, IEEE Transactions on. BME-30, Nr. 2*, p. 125–126, 1983.

[12] L. Rizzi, A. Farina, P. Galaverna, P. Martignon, A. Rosati, and L. Conti, "Scattering uniformity measurements and first reflection analysis in a large non-anechoic environment," in *123rd Convention of the Audio Engineering Society*, (New York), 2007.

[13] N. Aff, "Fractal dimension as a statistical property." https://nateaff.com/2017/06/14/fractal-dimension-as-a-statistical-property/, 2017. [Online; accessed 24-April-2023].

[14] M. Vorländer and E. Mommertz, "Definition and measurement of random-incidence scattering coefficients," *Applied Acoustics*, no. 60, pp. 187–199, 2000.

[15] A. Derheim, *Gekoppeltes Raytracing für Licht- und Schallausbreitung*. Stuttgart: Diplomarbeit, 2012.

[16] NORDTEST, *rough surfaces: Determination of the acoustic impedance*. 1999.

[17] W. Bartolomaeus, "Schallstreuung an achsenparallelen Zylindern," in *DAGA*, (München), 2018.